Available online at www.sciencedirect.com
SCIENCE DIRECT®
Journal of Nuclear Materials 355 (2006) 21–29
journal of nuclear materials
www.elsevier.com/locate/jnucmat

Volume changes in δ-plutonium from helium and other decay products

W.G. Wolfer *, Per Söderlind, A. Landa

Lawrence Livermore National Laboratory, University of California, P.O. Box 808, 7000 East Avenue, Livermore, CA 94550, USA

Received 5 December 2005; accepted 14 March 2006

Abstract

Small changes in volume are observed in plutonium, and several potential mechanisms have been proposed. In this paper, we provide a detailed theoretical analysis of volume changes due to the accumulation of helium and daughter products generated in the radioactive decay of plutonium. It is shown that volume changes in δ-phase plutonium caused by Am, U, and Np are significant and compensate to some degree the swelling from helium bubble formation and growth. Comparison with experimental results obtained so far suggests that the decay products dominate the rate of volumetric change in the long run.

PACS: 61.80.Az; 61.82.Bg; 81.30.Bx; 82.60.Lf; 89.20.Dd

1. Introduction

The radioactive decay of plutonium will over time change the composition of the material and also lead to slight changes in its specific volume. There are several possible contributions to dimensional changes [1]. First, at ambient temperatures the lattice parameter of gallium stabilized δ-Pu increases and reaches a new value after 2–3 years. As Chebotarev and Utkina have reported [3], this transient increase in lattice parameter increases with the gallium content, and it can be reversed by heating the material; after returning to ambient temperature, the lattice parameter increases again to its characteristic saturation value. Second, the accumulation of helium from the α-decay in the form of bubbles has been observed by transmission electron microscopy [2]. These bubbles are known to expand the external volume of the material that contains them. Third, a plutonium atom that undergoes a radioactive decay changes to a different actinide daughter product with a different atomic volume. A forth contribution may arise from voids created at high radiation doses. However, in samples with radiation damages up to 4 dpa, no evidence for void swelling has so far been found when examined by transmission electron microscopy [2]. Finally, plutonium is marginally kept stable in its δ-phase at ambient temperatures by small additions of gallium. If part of the δ-phase were to transform to a different phase, most likely to the α-phase, a volume contraction would occur. Long-term experimental

* Corresponding author. Tel.: +1 925 423 1501; fax: +1 925 423 7040.
E-mail address: wolfer1@llnl.gov (W.G. Wolfer).

0022-3115/$ - see front matter © 2006 Published by Elsevier B.V.
doi:10.1016/j.jnucmat.2006.03.018

studies are in progress to detect and measure precisely the sum of all possible dimensional changes, and some data have recently been published on a plutonium–gallium alloy enriched with the isotope ^{238}Pu [4]. Theoretical studies, however, must be carried out to quantify the different contributions. Here, we report only on our evaluation of the dimensional changes produced by all the decay products, including helium. The initial expansion of the lattice parameter that is reversible upon heating will be the subject of a forthcoming paper [26].

We begin, in Section 2, with a discussion of a typical isotopic composition of plutonium as employed in nuclear weapons, and of the various radioactive decay channels associated with the isotopes. Next, we describe in section 3 our determination of the partial molar volumes of the actinide decay products in the δ-phase of plutonium, followed in Section 4 by an evaluation of swelling caused by helium bubbles. In Section 5, we report our predictions of volume changes and compare it with experimental results. Our conclusions are briefly summarized in Section 6.

2. Production of actinide daughters and helium

Weapons-grade plutonium consists of a number of different isotopes. They are listed in Table 1 together with typical values of their initial concentrations in the second column. Actual concentrations vary somewhat for different weapon systems. In particular, the isotope ^{241}Pu has often decayed to ^{241}Am to some extent by the time a weapon is manufactured. Table 1 gives the decay chains in each row, starting with the parent nucleus on the left and proceeding to the final stable nucleus on the very right. Each of the isotopes has two decay channels. With the exception of ^{241}Pu, there is a α-decay leading to an intermediate uranium daughter. This daughter product will eventually decay by another α-emission to thorium. However, the half-life of the uranium daughter is so long that we may assume for the present analysis that it represents the final product. The other decay channel is the spontaneous fission of the plutonium nucleus. Again, however, the half-life for this nuclear reaction is so long that we may safely ignore it from further considerations. We note that the α-decay of ^{238}Pu has a short half-life of only 87 years. As a result, even small amounts of this isotope contribute significantly to the overall production of helium and radiation damage in nuclear stockpile materials.

As already mentioned, ^{241}Pu has an exceptional decay scheme and with a relatively short half-life of merely 14.63 years it decays either by electron or α-emission. However, the latter has a probability of less than 0.01%, and we may neglect this decay channel. The β-decay leads to an intermediate ^{241}Am nucleus which further decays with a half-life of 458 years to ^{237}Np.

We see that there are then only three daughter products, namely U, Am, and Np which need to be considered as solute elements affecting the alloy chemistry and the lattice parameter. Helium, being the other major decay product must be treated differently and separately.

Let us denote with x_I^0 the initial atomic fraction or abundance of the isotope with mass I, and with λ_I the decay constant. The atomic fractions of daughter product can then easily be evaluated [5] and are given by the equations

Table 1
Radioactive decay characteristics of plutonium isotopes

Parent isotope	Abundance (%)		Decay channel	Half-life years	Daughter isotope	Decay channel	Half-life years	End product
	WG	Spiked[a]						
^{238}Pu	0.02	7.38	α	87	^{234}U	α	2.5×10^{5}	^{230}Th
			Fission	5×10^{10}				
^{239}Pu	93.6	86.2	α	24 390	^{235}U	α	7×10^{8}	^{231}Th
			Fission	5×10^{15}				
^{240}Pu	5.9	5.52	α	6580	^{236}U	α	2.4×10^{7}	^{232}Th
			Fission	1.3×10^{11}				
^{241}Pu	0.44	0.15	β	14.63	^{241}Am	α	458	^{237}Np
			α (<.01%)	14.63	^{237}U	β	6.7 days	^{237}Np
^{242}Pu	0.04	0.057	α	3.8×10^{5}	^{238}U	α	5.4×10^{9}	^{230}Th
			Fission	7.4×10^{10}				

[a] WG stands for weapons-grade, and Spiked for material enriched in ^{238}Pu.

$$x_{\mathrm{U}}(t) = x^0_{238}(1-\mathrm{e}^{-\lambda_{238}t}) + x^0_{239}(1-\mathrm{e}^{-\lambda_{239}t}) + x^0_{240}(1-\mathrm{e}^{-\lambda_{240}t}) + x^0_{242}(1-\mathrm{e}^{-\lambda_{242}t}) \cong (x^0_{238}\lambda_{238} + x^0_{239}\lambda_{239} + x^0_{240}\lambda_{240} + x^0_{242}\lambda_{242})t, \tag{1}$$

$$x_{\mathrm{Am}}(t) = x^0_{241}\frac{\lambda_{241}}{\lambda_{241}-\lambda_{\mathrm{Am}}}(\mathrm{e}^{-\lambda_{\mathrm{Am}}t} - \mathrm{e}^{-\lambda_{241}t}), \tag{2}$$

$$x_{\mathrm{Np}}(t) = x^0_{241}\frac{1}{\lambda_{241}-\lambda_{\mathrm{Am}}} \times \{\lambda_{241}(1-\mathrm{e}^{-\lambda_{\mathrm{Am}}t}) - \lambda_{\mathrm{Am}}(1-\mathrm{e}^{-\lambda_{241}t})\}. \tag{3}$$

Given the long half-lives of the plutonium isotopes that decay to uranium, the increase in U is for all practical purposes a linear function of time, as is indicated in the second part of Eq. (1).

A helium atom is born in the decay sequence of every Pu isotope. However, for the ^{241}Pu decay, there is a temporary delay because the α-decay of Am is preceded by β-decay. The helium concentration is equal to the concentration of uranium and neptunium daughter products. Hence the equation

$$x_{\mathrm{He}}(t) = x_{\mathrm{U}}(t) + x_{\mathrm{Np}}(t). \tag{4}$$

Eq. (4) can easily be calculated using Eqs. (1) and (3).

The results are shown in Fig. 1 for the isotope abundances listed in the second column of Table 1. The delay of the helium production from ^{241}Pu is seen when the asymptotic production rate is extrapolated backwards as indicated by the dashed line. Disregarding this minor deviation we note that about 400 at. ppm (atomic parts per million) of helium is produced per decade in weapons-grade plutonium.

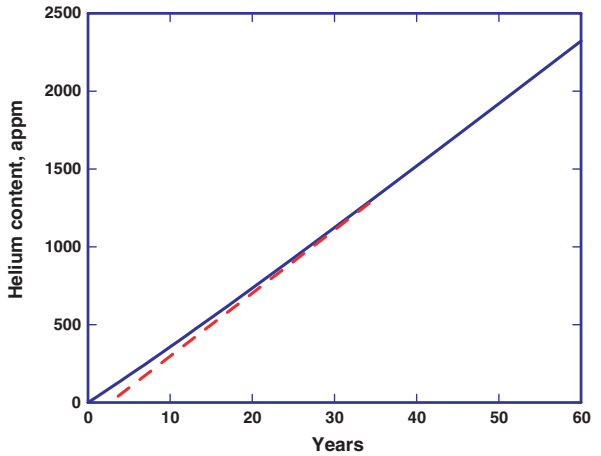

Fig. 1. Helium concentration as a function of time in weapons-grade plutonium, in atomic parts per million, for the isotope composition listed in Table 1 under column 'WG'.

Let us denote by $\overline{V}_I$ the partial molar volume of the daughter product which stems from the plutonium isotope with mass number I. The change in volume of the parent material, the Pu–Ga alloy in the δ-phase, due to the accumulation of other actinide daughter products, is then given by

$$\left.\frac{\Delta V}{V_0}\right|_A = x_{\mathrm{U}}(t)\frac{\overline{V}_{\mathrm{U}} - \overline{V}_{\mathrm{Pu}}}{\overline{V}_{\mathrm{Pu}}} + x_{\mathrm{Am}}(t)\frac{\overline{V}_{\mathrm{Am}} - \overline{V}_{\mathrm{Pu}}}{\overline{V}_{\mathrm{Pu}}} + x_{\mathrm{Np}}(t)\frac{\overline{V}_{\mathrm{Np}} - \overline{V}_{\mathrm{Pu}}}{\overline{V}_{\mathrm{Pu}}}. \tag{5}$$

The partial molar volumes of the three daughter products in δ-Pu are not all known. For Am, it can be obtained from experimental lattice-parameter measurements made on Pu–Am binary alloys [6].

3. Determination of partial molar volumes

In general, if $V(x_I)$ denotes the molar volume of a binary alloy with a daughter product content of x_I atomic fractions, the partial molar volumes for the two elements in a binary alloy are defined as

$$\overline{V}_{\mathrm{Pu}} = V(x_I) - x_I\left(\frac{\mathrm{d}V}{\mathrm{d}x_I}\right), \qquad \overline{V}_I = V(x_I) + (1-x_I)\left(\frac{\mathrm{d}V}{\mathrm{d}x_I}\right). \tag{6}$$

From these two equations we can form a parameter which we shall call the dilatation of the solute I in δ-Pu

$$\frac{\overline{V}_I - \overline{V}_{\mathrm{Pu}}}{V(x_I)} = \frac{1}{V(x_I)}\left(\frac{\mathrm{d}V}{\mathrm{d}x_I}\right). \tag{7}$$

In the limit of infinite dilution, $x_I \to 0$, the partial molar volume of plutonium becomes equal to the molar volume, V^0_{Pu}, of pure Pu in the particular phase of the alloy, and the dilatation is

$$\frac{\overline{V}_I}{V^0_{\mathrm{Pu}}} - 1 = \frac{1}{V^0_{\mathrm{Pu}}}\left(\frac{\mathrm{d}V}{\mathrm{d}x_I}\right)_{x_I=0}. \tag{8}$$

These are the parameters needed to evaluate the volume change of Eq. (5).

For cubic crystal phases the partial molar volumes are related to the lattice parameter $a(x_I)$, and the dilatation is given by

$$\frac{\overline{V}_I - \overline{V}_{\mathrm{Pu}}}{\overline{V}_{\mathrm{Pu}}} = \frac{3}{a(x_I)}\frac{\mathrm{d}a}{\mathrm{d}x_I}. \tag{9}$$

First-principles electronic structure methods can also be used to determine partial molar volumes. In the present paper, we employ two different

computational techniques. The most accurate method, which is also the most computer intensive, is an all-electron, full-relativistic (spin–orbit coupling is included), full potential linear muffin–tin orbitals (FPLMTO) method [7,8]. In the FPLMTO method one can approximate the $Pu_{1-x}I_x$ (I = Am, U, and Np) alloy with a large super-cell or an ordered compound. Because the ordered compound involves far less atoms, this is the more efficient approach and is used here. Söderlind [9] found that antiferromagnetic (AF) $L1_0$ type structure is the most energetically stable magnetic configuration for δ-Pu at $T = 0$ K. We used AF configuration for δ-Pu as well as for PuX compounds (Pu_3I ($L1_2$) and PuI ($L1_0$)) in the FPLMTO calculations. The equilibrium density (molar volume $V(x_I)$) was obtained from a Murnaghan fit [10] to about ten total energies calculated as a function of the atomic volume. The energy minimum determines then the molar volume $V(x_I)$. The assumption of antiferromagnetic spin ordering encounters widespread concerns among reviewers and readers alike in view of the fact that no magnetism is found in plutonium. While this is too complex an issue to deal with in this paper, we explain in Appendix A why this assumption can be made.

The FPLMTO method is very accurate but has two limitations. First, if n atoms are solute atoms and $(N - n)$ are solvent atoms, then $x = n/N$ can only assume discrete values. Second, periodic boundary conditions for the super-cell calculations imply an ordered compound rather than a random solution alloy. Furthermore, finding the volume of the super-cell with the lowest energy for an alloy does not eliminate all forces on the periodic boundaries. However, as is shown in the Appendix B, it will determine the correct molar volume of the alloy.

To allow calculations for solutes at arbitrary concentrations, another theoretical approach is employed. The calculations we have referred to as KKR–ASA are performed using the scalar-relativistic (spin–orbit coupling is neglected) spin-polarized Green's function technique based on the Korringa–Kohn–Rostoker (KKR) method within the atomic sphere approximation (ASA) [11,12]. The effect of compositional and magnetic disorder is treated by means of the coherent potential approximation (CPA) [13]. As was suggested in Ref. [14,15], at elevated temperatures δ-Pu is argued to be a disordered magnet or paramagnetic (PM) that upon cooling undergoes transformation to the AF structure with a mechanical destabilization and phase transition to a lower symmetry phase as the result. The PM state of δ-Pu and its alloys is represented by the disordered local moment (DLM) [16] incorporated within the CPA.

Americium and plutonium form a continuous solid solution in the face-centered-cubic (fcc) lattice structure. Lattice parameters for this binary alloy have been measured by Ellinger et al. [6], and the dilatation as determined from Eq. (9) is shown in Fig. 2. Landa and Söderlind [17] carried out first-principle calculations on Pu–Am alloys and also obtained values for the dilatation as shown in Fig. 2. The agreement between the computed and the experimental values for Am concentrations of 20% or less is excellent, and it confirms the proof in the Appendix B that the volume change caused by solutes in a finite solid are indeed equal to the change computed with periodic boundary conditions.

Fcc alloys of Pu–U or of Pu–Np do not exist at ambient conditions and their lattice parameters can therefore not be determined experimentally. Instead we have performed calculations for these alloys and the dilatations are shown in Figs. 3 and 4.

The dilatations for dilute solute concentrations are listed in Table 2.

These values strictly apply only to the corresponding binary alloys. Yet we intend to use them also for Pu–Ga–Am–U–Np alloys containing supersaturations of vacancies and self-interstitials. First, let us consider the effect of gallium. In a Pu–Ga alloy with 3 at.% gallium, the volume per atom is

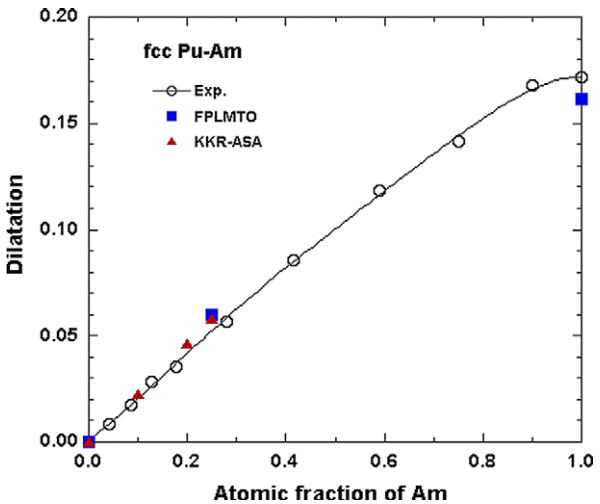

Fig. 2. Volume change in Pu–Am alloys with increasing Am content relative to the partial molar volume of δ-plutonium. The curve is a fit to the experimental data in Ref. [6].

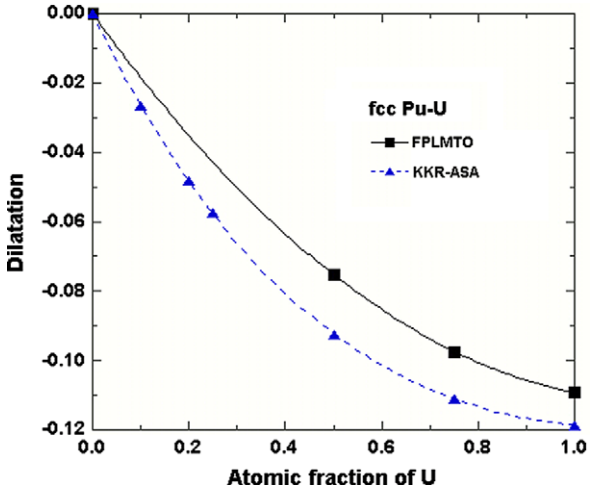

Fig. 3. Volume change in Pu–U alloys with increasing U content relative to the partial molar volume of δ-plutonium.

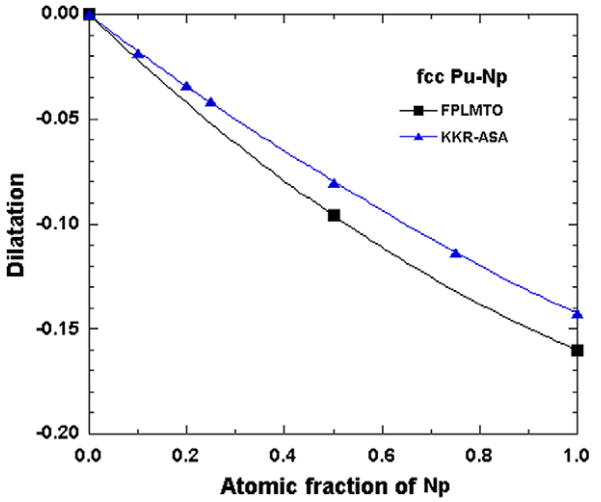

Fig. 4. Volume change in Pu–Np alloys with increasing Np content relative to the partial molar volume of δ-plutonium.

Table 2
Dilatations for Am, U, and Np in δ-Pu at infinite dilution

$(\overline{V}_I/\overline{V}^0_{Pu}) - 1$	Experiment	FPLMTO	KKR–ASA
Am	+0.2338	+0.2640	+0.2206
U		−0.1920	−0.2480
Np		−0.2240	−0.1763

smaller by about 2% than the atomic volume of plutonium in the pure δ-phase. A correction of this magnitude should be made to the parameters given in Table 2. However, such a correction is small compared to the 30% difference obtained with the two computational methods. The mutual effect of the other actinide solutes on their respective dilatation values is even smaller since their combined concentration remains below 0.5 at.%. The concentration of vacancies or self-interstitials maintained by radiation damage at ambient temperature is estimated to be less than 0.1 appm, and it will not affect the partial molar volume of solute atoms.

In summary, the concentrations of actinide daughter products is so small that a linear superposition of their individual contributions to the density is justified, and the effect of gallium can be eliminated when computing relative changes in density or volume, as expressed by Eq. (5).

4. The effect of helium on density

The helium generated by the α-decay either resides in bubbles or is still in solution. The two populations with concentrations x^{B}_{He} and x^{S}_{He} make the following contribution to the volume change:

$$\left.\frac{\Delta V}{V_0}\right|_{He} = x^{B}_{He}(t)\frac{\overline{V}^{B}_{He}}{\overline{V}^{0}_{Pu}} + x^{S}_{He}(t)\frac{\overline{V}^{S}_{He}}{\overline{V}^{0}_{Pu}}. \quad (10)$$

In a recent paper, Schwartz et al. [2] report on the examination by transmission electron microscopy of old plutonium samples ranging in age from 16 to 42 years. Measuring both bubble diameters and bubble densities by transmission electron microscopy, the bubble volume fraction was determined and found to increase linearly from 0.01% to 0.03%. The evolution of the bubble density was modeled with rate equations describing the irreversible aggregation of diffusing helium atoms [18]. Predicted and observed bubble densities could be made to agree by selecting an appropriate helium diffusion coefficient. It was found that an activation energy for helium migration of 0.72 eV resulted in the most satisfactory agreement. A consequence of this model is that very low concentrations of helium in solution are predicted, after just a few months of aging. For example, the helium in solution drops to about 1 ppb (part per billion) at 300 K and to about 1 ppm (part per million) at 200 K. We may therefore neglect the second term in Eq. (10) entirely, and assume that all the helium produced resides in bubbles.

The ratio of the partial molar volumes of plutonium and of helium in bubbles, i.e. $\overline{V}^{0}_{Pu}/\overline{V}^{B}_{He}$, is equal to the number of helium atoms which occupy within a bubble the volume vacated by one

plutonium atom. This helium to vacancy ratio, or He/Vac., is found to be between 2 and 3.

Two independent determinations of this ratio have been made. First, the image of the bubble diameters of about 1 nm as seen in the transmission has been shown to be about 20% smaller than the real diameters of such small bubbles [19]. As a result, the bubble volume fraction, as computed from the visible images, is larger by a factor of 1.73. When the known helium concentration in the aged Pu samples is divided by this actual bubble volume, a He/Vac. ratio between 2 and 3 is obtained.

The second determination of the helium density in bubbles was obtained by Sterne et al. [20] with positron annihilation lifetime measurements on old plutonium samples and with first-principles calculations of annihilation rates of positrons trapped in vacancy clusters, voids and helium bubbles. These calculations have shown that calculated positron lifetimes in old plutonium samples agree with the measured values of 180–200 ps if the He/Vac. ratio is between 2 and 3 for bubbles with diameters between 1 and 2 nm, the sizes inferred from transmission electron microscopy.

We note that values for He/Vac. of around 2 have been found for helium bubbles formed by tritium decay in metals such as Pd [19], Nb, Lu, Zr, V, Ta, Y, and Sc [21–23]. The somewhat smaller number can be explained by the smaller atomic volume for these metals compared to the larger value of 0.025 nm^3 for δ-Pu.

5. Results

The total volume change can now be computed as the sum of Eqs. (5) and (10). Let us first consider the contribution to the volume change by the actinide daughter products in weapons-grade material. Eq. (5) gives the curves labeled as 'Actinides' in Fig. 5. Here, the experimental value for the dilatation of Am has been used in both cases. The build-up of Am is the reason for the steep initial volume increase. However, after about 30 years the further generation of Am diminishes and the production of uranium reverses the volume expansion to a contraction. The two different predictions arise predominantly from the different partial molar volumes computed for U with the FPLMTO and the KKR–ASA method. When we add the contribution of helium obtained with Eq. (10) and for He/Vac. = 2.5, the upper curves shown in Fig. 5 are obtained. We see that the volume increase caused

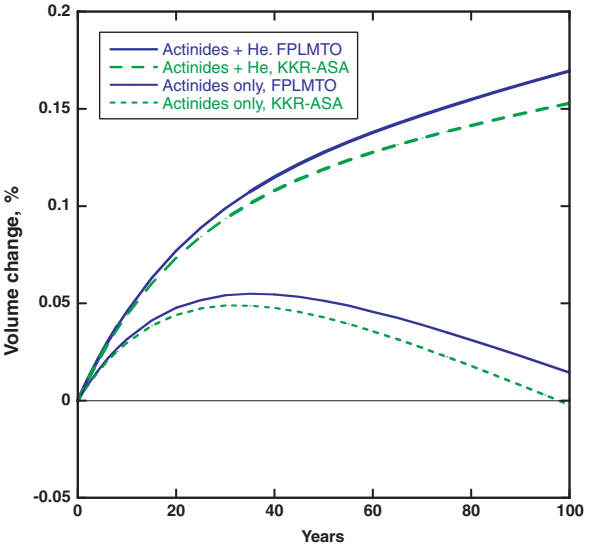

Fig. 5. Relative volume change due to the in-growth of actinide daughter products (lower curves) plus helium (upper curves) for weapons-grade plutonium (see main text).

by helium bubbles is significantly compensated by the volume contraction caused by the accumulation of U and Np. To further assess the degree of this compensation, we consider the greatest and smallest volume change predicted. Choosing He/Vac. = 2 and the partial molar volumes computed with the FPLMTO method gives the largest volume change, while He/Vac. = 3 together with the KKR–ASA results gives the lower volume change. Both are shown in Fig. 6 after adding a constant value of 0.03% for the transient lattice parameter expansion, estimated from the values obtained by Chebotarev and Utkina [2]. We also display in Fig. 6 measured volume changes of old plutonium samples extracted from retired nuclear weapons [24]. These volume changes are derived from two measurements of immersion densities made many years apart and in different laboratories. The initial density measurements were performed on batches of plutonium components after they were fabricated, but no records were kept on the density of an individual component. Therefore, the densities of the small samples extracted from these components can only be compared to the average initial density of a batch. Hence the large scatter in the data. The comparison of our theoretical predictions with these experimental data only demonstrates that there is no discrepancy. But it does not constitute at all a validation of the theory. More accurate measure-

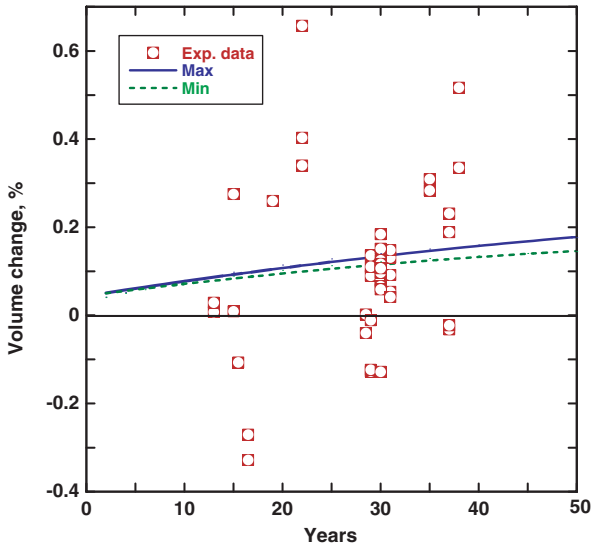

Fig. 6. Relative volume change in weapons-grade plutonium. The solid curve is a prediction for a helium density in bubbles of two helium atoms per vacant site and the dashed curve for 3. Experimental data are from samples extracted from retired nuclear weapons. The wide scatter is explained in the text.

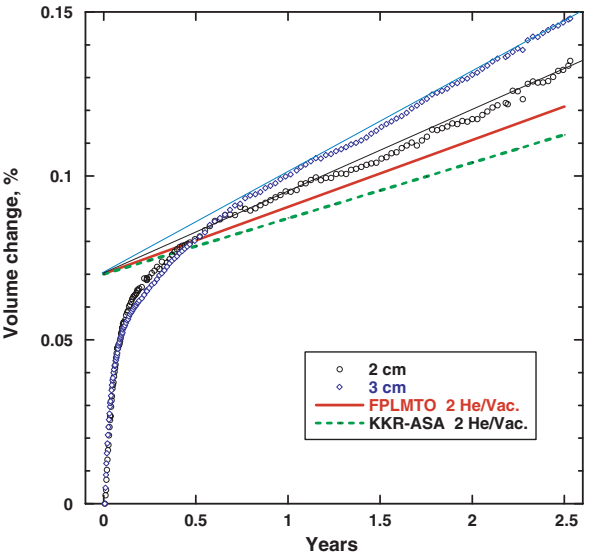

Fig. 7. Relative volume change for spiked material with a composition given in Table 1 under column 'Spiked'. A comparison with predictions is made only for the steady state part of the expansion after the transient, and assuming a helium density in bubbles of two helium atoms per vacant site.

ments are needed and are in progress using small specimens of plutonium enriched in ^{238}Pu.

Some preliminary data have recently been published by Chung et al. [25] on length changes of plutonium–gallium alloy samples that were made with a 7.5 at.% of ^{238}Pu, but were otherwise similar in isotope composition as given in the third column of Table 1. These so-called spiked samples accelerate the overall α-decay by a factor of about 17. We show in Fig. 7 the volume changes in two of these samples aged at 35 °C, assuming that these changes are three times the measured length changes. The initial transient expansion will be explained in a forthcoming paper. Here, we focus on the steady state expansions which Chung et al. [4] have also measured on samples held at 50 °C and 65 °C and found to be very similar to those at 35 °C. As indicated in Fig. 7, the steady state expansion can be fit to straight lines, and when extrapolated to time zero, give a saturation value of 0.07% for the transient part of the volume expansion. The sample with a length of 2 cm expands at a lower rate than the 3 cm long sample. Possible reasons for this difference are discussed by Chung et al. [4].

The volume changes calculated for these spiked samples turn out to be straight lines, and they are shown in Fig. 7 displaced by the saturation value for the transient expansion. The case shown is for a helium density in bubbles of 2.0 He/Vac. It would be possible to match the slope of the theoretical predictions by choosing a somewhat smaller value for the helium density in bubbles. However, the experimental slopes also have some uncertainty, as discussed by Chung et al. [4], that needs to be resolved before reaching a definite conclusion.

We note that spiked samples do not display the steeper initial expansion due to Am as predicted for weapons-grade material. The expansion in spiked samples is dominated by the helium and U productions from the decay of ^{238}Pu, and both are increasing almost linearly with time.

6. Summary and conclusions

We have presented a theoretical model for the dimensional changes in aging δ-Pu due to creation of actinide daughter products and due to helium accumulation. By performing first-principles calculations we have obtained the volume dilatation associated with the existence of U, Np, and Am in δ-Pu. This, combined with the known half-life times of the daughter products and the measured helium density in bubbles, has enabled us to predict the volume change in δ-Pu as it ages. Our theoretical predictions compare very favorably with experimental

expansion data beyond the initial transient. This initial transient is caused by a different process, and it is treated in a forthcoming publication [26].

Acknowledgements

This work was performed under the auspices of the US Department of Energy by the University of California Lawrence Livermore National Laboratory under contract W-7405-Eng-48.

Appendix A

Spin-polarized density functional theory (SP DFT) has been applied to all the phases of plutonium [27] with good success. It reproduces the crystal structures and their densities as well as the correct order of their ground state energies. These calculations are performed assuming a particular ordering of the spin magnetic moments of 5f-electrons and varying the size of the unit cell. In this manner, a minimum energy is found at a certain size of the unit cell for the assumed spin configuration. Next, other spin configurations are tested until the one is found that gives the lowest possible energy. Söderlind and Sadigh [27] have discovered a remarkable empirical rule that enables one to pick the optimum spin configuration, and very few spin configurations need to be sampled. For the δ-phase, it is found that the anti-ferromagnetic spin configuration with large spin magnetic moments generates the lowest energy and the largest atomic volume. The latter result agrees with experimental facts while the former is in apparent contradiction with all magnetic measurements. We have recently extended [28] the application of SP DFT to gallium-stabilized δ-plutonium and the α′-phase. Again, very satisfactory results are obtained for structural properties and thermodynamic properties at absolute zero of temperature. Yet again, spin magnetic moments are found and antiferromagnetic ordering gives the lowest, and correct energies.

Clearly, there is something missing in the SP DFT when one has to deal with magnetic properties, and this does not come as a surprise to theorists who fully understand the foundation of this theory. A more detailed discussion of the issues is given in the introduction of Ref. [28]. Here, we can only touch briefly on some of them:

1. Magnetic moments may be shielded by the Kondo effect.
2. Correlated fluctuations of spin configurations may eliminate a Curie–Weiss behavior.
3. Spin moments may be exactly cancelled by an anti-parallel orbital moments with the same magnitude.

Point 3 is strongly suggested by the SP DFT whereas 1 or 2 cannot be addressed by this approach. The theory must be supplemented, and different models are being developed. However, none of these has the rigorous foundation of the SP DFT nor its successes in many areas of physics and chemistry.

Appendix B

The introduction of a solute atom into a crystal will in general produce elastic stresses $\sigma_{ij}(\boldsymbol{r})$ in the surrounding host. For cubic crystals, the volume change associated with these stresses is ∫given by [29]

$$\Delta V = \frac{1}{3K}\left\{ \oiint x_k \sigma_{kl} n_l \, \mathrm{d}S + \int\int\int x_k f_k \, \mathrm{d}^3 r \right\}, \tag{A.1}$$

where K is the bulk modulus, $\boldsymbol{n}$ is a unit vector on the surface pointing outwards, and the stresses are obtained by solving the equations of elasticity

$$\sigma_{ij,j} + f_i = 0. \tag{A.2}$$

The usual summation convention is used for repeated indices, and an index after a comma indicates partial differentiation. The forces $\boldsymbol{f}(\boldsymbol{r})$ are the ones generated by the solute atom on the surrounding host atoms prior to their relaxation. In a crystal of finite extent, the stresses must also satisfy the boundary condition $\sigma_{kl} n_l = 0$ on the external surface of the crystal, and hence, the first integral vanishes.

For electronic structure calculations as performed here, periodic boundary conditions are employed, and the stresses are different than those obtained in a finite crystal with stress-free boundaries. However, when the periodic cell volume is changed such that the crystal energy reaches its minimum value, this implies that the sum of all forces on the relaxed cell boundary vanishes. In this case, the first integral in (A.1) vanishes again. Hence, within the linear theory of elasticity, or the harmonic approximation of crystals, the volume change obtained with relaxed, periodic boundaries is identical to the volume change in a finite crystal with stress-free boundaries, even though the stresses within the relaxed cell differ from those of the finite

cell. Unfortunately, because of this difference, the strain energies associated with the solute atoms are not the same for the two cases.

References

[1] J.C. Martz, A.J. Schwartz, J. Metals 55 (2003) 19.
[2] A.J. Schwartz, M.A. Wall, T.G. Zocco, W.G. Wolfer, Philos. Mag. 85 (2005) 479.
[3] N.T. Chebotarev, O.N. Utkina, in: H. Blank, R. Lindner (Eds.), Plutonium and other Actinides, 1975, North-Holland, Amsterdam, 1976, p. 559.
[4] B.W. Chung, S.R. Thompson, C.H. Woods, D.J. Hopkins, W.H. Gourdin, B.B. Ebbinghaus, J. Nucl. Mater., submitted for publication.
[5] I. Kaplan, Nuclear Physics, 2nd Ed., Addison-Wesley, Reading, Mass, 1963, Chapter 10.
[6] F.H. Ellinger, K.A. Johnson, V.O. Struebing, J. Nucl. Mater. 20 (1966) 83.
[7] J.M. Wills, B.R. Cooper, Phys. Rev. B 36 (1987) 3809.
[8] D.L. Price, B.R. Cooper, Phys. Rev. B 39 (1989) 4945.
[9] P. Söderlind, Eur. Phys. Lett. 55 (2001) 525.
[10] F.D. Murnaghan, Proc. Natl. Acad. Sci. USA 30 (1944) 244.
[11] I.A. Abrikosov, H.L. Skriver, Phys. Rev. B 47 (1993) 16532.
[12] A.V. Ruban, H.L. Skriver, Comput. Mater. Sci. 15 (1999) 119.
[13] J.S. Faulkner, Prog. Mater. Sci. 27 (1982) 1.
[14] P. Söderlind, A. Landa, B. Sadigh, Phys. Rev. B 66 (2002) 205109.
[15] A. Landa, P. Söderlind, J. Phys.: Condens. Mater. 15 (2003) L371.
[16] B.L. Györffy, A.L. Pindor, G.M. Stocks, G.M. Staunton, H. Winter, J. Phys. F: Met. Phys. 15 (1985) 1337.
[17] A. Landa, P. Söderlind, J. Alloys Comp. 376 (2004) 62.
[18] C.M. Schaldach, W.G. Wolfer, Kinetics of helium bubble formation in nuclear and structural materialsThe Effects of Radiation on Materials: 21st International Symposium, 1447, ASTM STP, 2004, p. 479.
[19] D.S. Gelles, R.A. Causey, K. Hertz, D.F. Cowgill, R. Schäublin, Bubble microstructures in helium injected palladium foilsThe Effects of Radiation on Materials: 21st International Symposium, 1447, ASTM STP, 2004, p. 492.
[20] P. Sterne, J. van Ek, R.H. Howell, Comp. Mater. Sci. 10 (1998) 306.
[21] T. Schober, C. Dieker, R. Lässer, H. Trinkaus, Phys. Rev. B 40 (1989) 1277.
[22] O. Blaschke, J. Pleschiutschnig, R. Glas, P. Weinzierl, Phys. Rev. B 44 (1991) 9164.
[23] M. Prem, G. Krexner, J. Pleschiutschnig, J. Alloys Comp. 356&357 (2003) 683.
[24] B.B. Ebbinghaus, L. Morales, provided the unpublished data.
[25] We thank B.W. Chung for making available the more recent expansion data.
[26] W.G. Wolfer, B. Oudot, N. Baclet, J. Nucl. Mater., submitted for publication.
[27] P. Söderlind, B. Sadigh, Phys. Rev. Lett. 92 (2004) 185702.
[28] B. Sadigh, W.G. Wolfer, Phys. Rev. B 72 (2005) 205122.
[29] J.D. Eshelby, Solid State Phys. 3 (1956) 79.